

# Tumor Segmentation in Multimodal Brain MRI Using Deep Learning Approaches

Waleed Al Shehri<sup>1†</sup> and Najlaa Jannah<sup>2††</sup>,  
[washehri@uqu.edu.sa](mailto:washehri@uqu.edu.sa) [nmjannah@uqu.edu.sa](mailto:nmjannah@uqu.edu.sa)

Department of Computer Science, College of Computer in Al-Lith, Umm Al-Qura University  
Makkah, Saudi Arabia

## Abstract

A brain tumor forms when some tissue becomes old or damaged but does not die when it must, preventing new tissue from being born. Manually finding such masses in the brain by analyzing MRI images is challenging and time-consuming for experts. In this study, our main objective is to detect the brain's tumorous part, allowing rapid diagnosis to treat the primary disease instantly. With image processing techniques and deep learning prediction algorithms, our research makes a system capable of finding a tumor in MRI images of a brain automatically and accurately. Our tumor segmentation adopts the U-Net deep learning segmentation on the standard MICCAI BRATS 2018 dataset, which has MRI images with different modalities. The proposed approach was evaluated and achieved Dice Coefficients of 0.9795, 0.9855, 0.9793, and 0.9950 across several test datasets. These results show that the proposed system achieves excellent segmentation of tumors in MRIs using deep learning techniques such as the U-Net algorithm.

## Keywords:

*Brain Tumor Segmentation, MICCAI BRATS, FLAIR, MRI Modalities, U-Net, Dice Coefficient.*

## 1. Introduction

The human brain is a sensitive body organ consisting of billions of cells. According to the National Cancer Institute [2], normal cells in the human body grow, become old, and die. After that, new cells take their place when the body needs them. But when cancer occurs in the body, this process is disturbed; cells remain alive, divide, and spread into other body tissues resulting in a tumor.

In general, there are two types of tumors: malignant and benign. A malignant tumor divides and can spread through the blood or lymph system to different positions in the body to make new tumor cells [3]. On the other hand, a benign tumor does not divide or spread and can be removed from the body easily. Consequently, an early tumor diagnosis is critical as it could save people suffering

and dying from cancer due to a late diagnosis of the disease. Unfortunately, it takes a lot of time when an expert identifies if a patient has a tumor or not and, if so, where it is located manually [12]. Therefore, experts often analyze magnetic resonance images (MRIs) to detect tumors. MRIs are one image of a patient's brain to visually identify tumors' existence. They are primarily used in neurology and neurosurgery. The brain, spinal cord, and anatomy of vascular tissues can be easily viewed through this imaging technology.

The main advantage of this technology is that it provides a 3D view of a location or area of concern. For example, the brain can be viewed from axial, sagittal, and coronal orientations. The axial view is the top side view of the brain, the sagittal view is the left or right-side view of the brain, whereas the coronal view is the back side view of the brain. MRI has various modalities, but [1] discussed four modalities: T1, T1C, T2, and FLAIR [1]. Each has a specific purpose, but the most common use of T1, T1C, and T2 are understanding the brain's structuring to detect edema or necrosis. In contrast, the FLAIR imaging sequence is routinely used to detect tumor tissues in the brain.

The main challenge is segmenting the brain's tumorous region by analyzing an MRI image. Analysis can be categorized into manual, semi-automatic, and fully automatic. In the manual method, neurologists manually view and analyze the brain MRIs and highlight the tumorous area if found. In the second method of tumorous segmentation, human experts and computing software are involved. The human expert inputs the system, whereas the software processes the information and returns results to the human expert who analyzes the results. However, a semi-automatic method has drawbacks because every expert can change the output results based on input parameters.

On the other hand, the fully automatic method does not involve a human expert. Instead, the method includes image processing and machine learning algorithms to

---

Manuscript received August 5, 2022

Manuscript revised August 20, 2022

<https://doi.org/10.22937/IJCSNS.2022.22.8.42>

segment the image and then classify normal and tumorous cells. This method's main challenge is handling different sizes, shapes, and irregular boundaries in the brain images [1]. Therefore, Automatic Brain Tumor segmentation saves time and gives faster results than the abovementioned techniques.

The system proposed in this study is an automatic brain tumor segmentation system that uses the deep learning model U-Net for tumor segmentation in the state-of-the-art dataset BRATS 2018 [1]. The main challenge we addressed in this study is how to segment the tumorous region from brain MRIs accurately. The proposed system accurately addresses the tumorous area, tumor size, and tumor shape and identifies the tumor boundaries. The main focus is the segmentation of brain tumors in MRIs.

The paper is organized as section (II) discusses the Literature review, section (III) elaborates on the materials or dataset used in the proposed system, and section (IV) addresses the proposed research methodology. Finally, the last section (V) consists of the results and discussion.

## 2. Literature Review

Muhammad et al. [4] proposed an automatic technique for brain tumor segmentation using MRI. They used a super pixel-based method for image segmentation, and the features were extracted manually via statistical, texture, fractal, and curvature features. A randomized classifier was applied to classify between normal and abnormal superpixels. Their proposed model was evaluated using the BRATS 2012 dataset with the FLAIR sequence. They achieved a Dice score of 0.88. However, the feature-based approaches always take time to compute the feature vector first and then feature selection. Normally various features are missed during computation.

Rehman et al. [5] proposed a binary tumor classification method (tumor/non-tumor). Their approach used the superpixel segmentation method to partition the image into small patches. First, they extracted statistical, texture, and fractal features from segmented images. Then, they applied three different classifiers to classify the superpixels: Support Vector Machine (SVM), AdaBoost, and Random Forest (RF). They found that RF performs better with a precision value of 5% over the BRATS 2012 dataset with FLAIR images. Their approach focused on classifying tumor/no-tumor but needs to give a solution first in segmentation. After successful segmentation, classification will be the best approach.

Khan MA et al. [6] introduced a brain tumorous part segmentation approach. First, the tumor intensity is enhanced after image acquisition. Next, the tumor is

segmented, and the marker-based watershed segmentation method is used to extract shape, texture, and point features. They used the chi-square approach to select 70% of high-priority features at the feature selection step. Finally, SVM was used to classify the images as tumorous or non-tumorous. The proposed method was trained and tested upon three different datasets of FLAIR images from Harvard, BRATS 2013, and privately collected from the hospital. The reported accuracy against these datasets was 98.17%, 98.88%, and 98.50%, respectively. A tumorous area was not detected, which is still a crucial problem due to cell movement.

A method proposed by Rajan, P.G, et al. [7] classifies normal and abnormal images and the volume of detected tumors. First, the proposed applied pre-processing techniques enhance the image intensity. Then k-means and Fuzzy C-Means clustering algorithms are used to generate clusters of images. Features are extracted from the clustered images, which are passed to the SVM classifier that categorizes the images as normal or abnormal. Next, the abnormal images are segmented through active contour by level set (ACLS). Finally, intensity adjustment is made, and the tumor area and volume are computed from the abnormal images. The tested dataset consists of 40 slices collected privately.

Himaja and Lingaraju [8] focused on finding the tumor region or segmentation and checking whether it is benign or malignant. The whole process follows the following steps: (1) pre-processing of the images to remove noise, (2) segmentation to find the area of interest, (3) feature extraction, and (4) classification using a neural network. The proposed model results are 93.33% accuracy, 96.6% specificity, 93.33% sensitivity, and 94.44% precision. In addition, they argue that their algorithm performs better than the AdaBoost, classifying the images into three types (normal, benign, and malignant) with an accuracy of 89.90%. In their study, 60 MRI images were collected privately to train and test the proposed model privately.

Nooshin and K. Miroslav [9] work on brain segmentation, detecting tumorous areas, and evaluating the efficacy of statistical features over Gabor features because they experimented on these features. The algorithm uses mutual information from two hemispheres of the brain. When an image slice having a tumor is found, it is segmented to delineate the tumor area. They trained and tested the model over the BRATS 2013 standard dataset. Furthermore, they used a few features as various feature types can be calculated.

Our analysis of the previous literature shows that most studies are based on relatively old and small datasets and

use models with relatively low precision. Various techniques calculate few features; however, more rich features could be extracted with deep learning approaches. By studying these previous results and other applicable techniques, we decided to implement deep learning techniques for segmentation on the state-of-the-art dataset MICCAI BRATS 2018. Deep learning models like Convolutional Neural Networks (CNN), Recurrent Neural Networks (RNN), and U-Net have already been suggested for segmentation and require large amounts of data. However, MICCAI BRATS includes other datasets, BRATS 2012 to BRATS 2020. Consequently, providing large public MRI datasets.

We proposed an automatic brain tumor segmentation system based on the research study. This system is based on deep learning approaches to segment the tumorous area and identify the tumor boundaries accurately. The details are given below for the proposed system methodology.

### 3. Materials

There is a variety of open-source datasets for research on brain tumor segmentation. The most commonly used nowadays is MICCAI BRATS. We have collected a multimodal MRI dataset for brain tumor segmentation from the BRATS 2018 challenge [10]. The dataset provides an axial view with four sequences, as discussed in detail below. The following subsections present some important points about the BRATS 2018 dataset.

#### MICCAI BRATS Characteristics

**Data Modalities.** All the volumes in the BRATS 2018 were available in the form of neuroimages named NifTI (.nii.gz) containing different modalities like T1, T2, T1Gd, and FLAIR. However, various techniques [13] used the FLAIR sequence only for experimental analysis because it has spatial visibility.

**Data Labels.** The BRATS dataset already defined three labels in their research paper [1]. The labels are enhancing tumor (labeled 4), edema (labeled 2), necrotic tumor, and tumor that is non-enhancing core (labeled 1), with label 0 used for the remaining regions.

**Data Volume:** Whole data was skull stripped; we transformed all images into one mm<sup>3</sup> resolution, the same for all other datasets. The BRATS 2018 dataset has two main folders: HGG (High-Grade Glioma), which has 210 volumes of patient data, and LGG (Low-Grade Glioma), which has only 75 volumes of patient data. Each volume has MRI scans of the specific patient; the folders or volumes have four modalities, as mentioned above.

There is also ground truth for each volume inside each volume, and the NifTI file consists of four modalities and one ground truth for each modality.

**Data Format:** There are various solutions to read and convert the NifTI (.nii.gz) files into a NumPy 3D array. However, because all the volumes have NifTI files, it is challenging to compute raw data, and we apply pre-processing as discussed in the proposed methodology section.

## 4. Proposed Research Methodology

We proposed an automatic brain tumor segmentation from the MRI using deep learning techniques to find tumors as instantly and accurately as possible. The following subsections describe the steps performed during the research and development of the proposed system. Each step described what we implemented in the system.

### 4.1 Data Pre-Processing

The proposed data pre-processing approach helps deal with the large volume of data and easily passes the NumPy arrays into the deep learning algorithm. The pre-processing has the following steps:

**Step-01:** We collected the MRI scans for each patient and then combined all the volumes to store the data in an array. The basic purpose was to create NumPy arrays. The NumPy array is used for further processing in the system. The size for the array is denoted (N, S, N1, X), where parameters are denoted as:

N = Number of HGG/LGG datasets or volumes

S = Slice/image size

N1 = Total 2D slices from the MRI 3D each volume

X = Number of modalities or sequences

**Step-02:** We handled the HGG and LGG volumes one by one. The purpose was to get a 3D volume (N, 155,240,240,4). Since HGG had data or volumes for 210 patients and LGG had volumes for 75 patients, there was a need to distribute HGG volumes into three equal parts of N= 70. Therefore, we used these sets to be divided based on N values for HGG and LGG volumes.

**Step-03:** In this step, we pre-processed all the given data separately. All the slices did not show the tumor area, so we removed unnecessary slices from the volumes. We used only slices 30 to 120 for all the data files. The final shape was extracted as (N1,240,240,4). The exact form was extracted for the ground truths. As for the HGG volume, the value for N1 was  $90 \times 70 = 5600$ , and for the LGG volumes, N1 was  $90 \times 75 = 6750$ .

**Step-04:** The final experimental dimension had the optimum value (N1,192,192,4), and we used this shape for all the data files.

**Step-05:** In the last pre-processing step, we divided the data into three sets: a training set (60%), a validation set (20%), and a testing set (20%). This data pass to the proposed system for further computation.

**4.2 Proposed Model**

We adopted U-Net [14] deep learning model for the tumorous segmentation. U-Net is a convolutional neural network architecture for fast and precise image segmentation, specifically in medical imaging.

Figure 1 illustrates the proposed U-Net architecture for tumor segmentation. All the steps play an important role in segmentation, starting from the input layer, through the convolution layer and pooling, and finally to the segmented results. U-Net model has various convolution operations in each layer, improving the segmentation of the tumor. Furthermore, it has a multi-channel feature map, and many channels are generally shown at the architecture's top. As figure 1 shows, the x-y size is shown on the lower-left edge of the box, with some boxes showing the feature maps. The arrows denote the different operations.

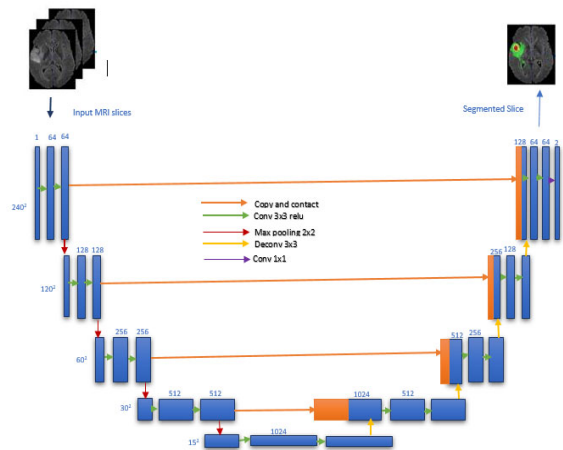


Fig 1. The Proposed system using U-net algorithm.

The illustration for tumor segmentation as our purpose is shown in figure 1 to get the accurately segmented area of the MRIs. Although the U-Net algorithm is the improved form of CNN, and it is best to fit for the segmentation of the image dataset, in our approach, we deal with it from the ground level using all possible layers necessary.

Our proposed approach updates the existing U-Net and adds additional layers to get the best classifier. More

details layers are used with the required parameters and the following steps performed in the model. Input images/slices pass to the model, convolution performed for each layer and applied max pooling for the better resolution of segment tumor. By increasing the number of layers in the U-Net algorithm, it tends to increase the resolution of outputs. As our problem is based on the localization of the tumorous area first, and then it segments out the tumorous area in the MRIs, it combines the output with the very high-resolution output.

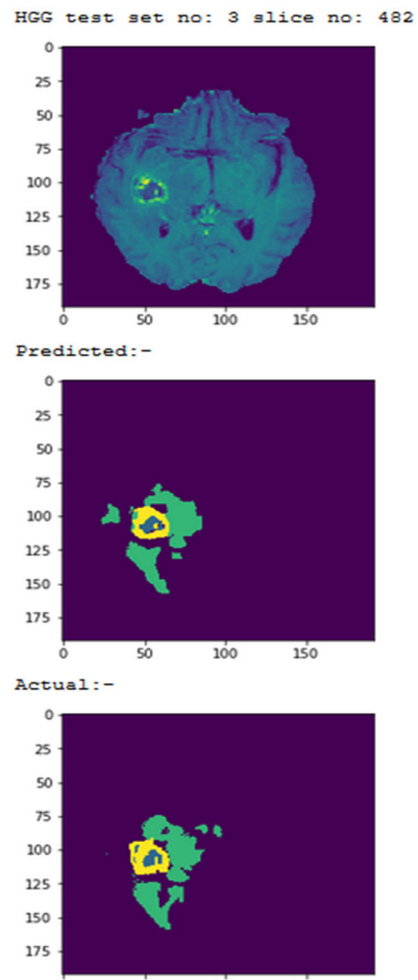


Fig 2. HGG Test Slice 482 Pictorial results for the normal, predicted by the proposed system and actual (ground truth).

**5. Results and Discussion**

The Proposed system outperformed after applying the proposed methodology to the BRATS 2018 dataset. The

Pictorial views of the HGG and LGG volumes are shown in figure 2 and figure 3. Figure 2 and figure 3 show an actual image (slice), the ground truth of that slice, and the predicted result.

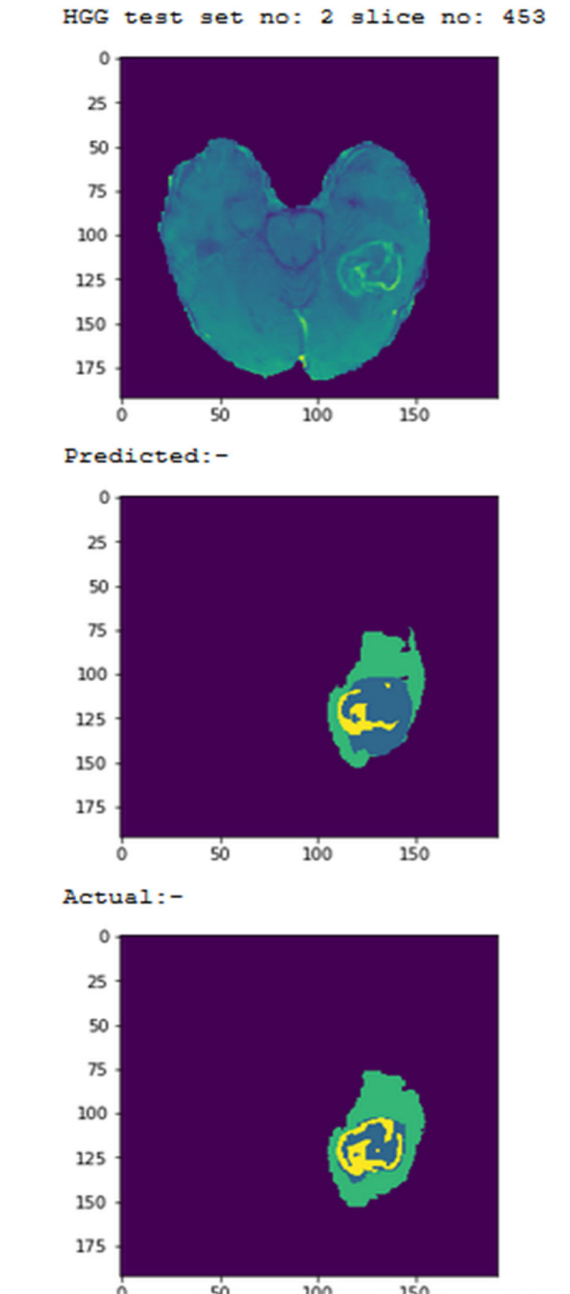
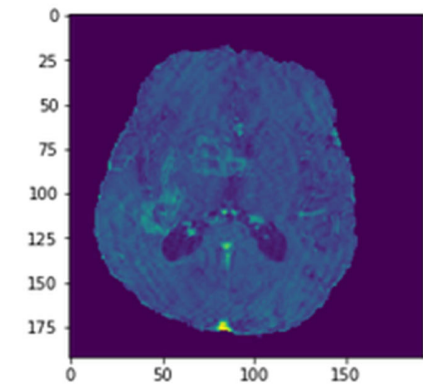
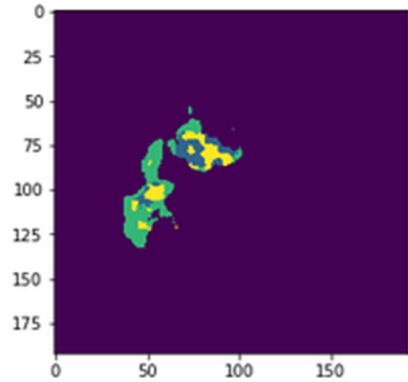


Fig. 3 HGG Test Slice 453 Pictorial results for the normal, predicted by the proposed system and actual (ground truth).

HGG test set no: 1 slice no: 499



Predicted:-



Actual:-

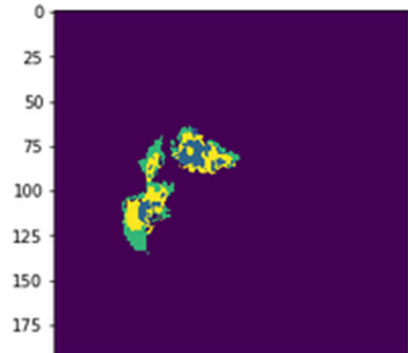


Fig. 4 HGG Test Slice 499 Pictorial results for the normal, predicted by the proposed system and actual (ground truth).

### 5.1 Pictorial Results for HGG Volumes

The results shown in Figures 2, 3, and 4 are a few samples to show the model’s accuracy and the physical view of the results. Again, the actual slice is given at the top, the predicted results in the middle, and the bottom shows the actual results or ground truth.

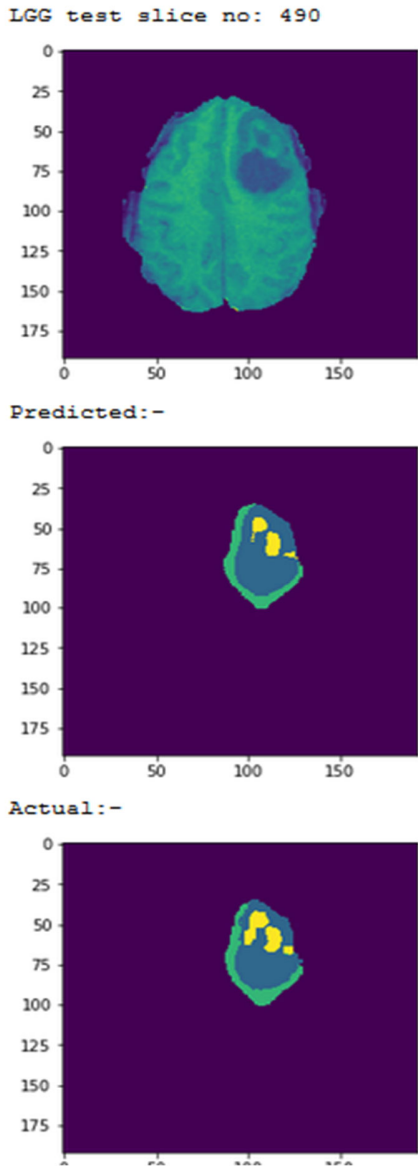


Fig. 5 LGG Test Slice 490 Pictorial results for the normal, predicted by the proposed system and actual (ground truth).

**5.2 Pictorial Results for LGG Volumes**

The results shown in Figures 5 and 6 are a few samples to show the model’s accuracy and physical view. The actual slice is given at the top, the middle image provides the predicted results, and the bottom shows the actual results or ground truth. These are results for the LGG volumes.

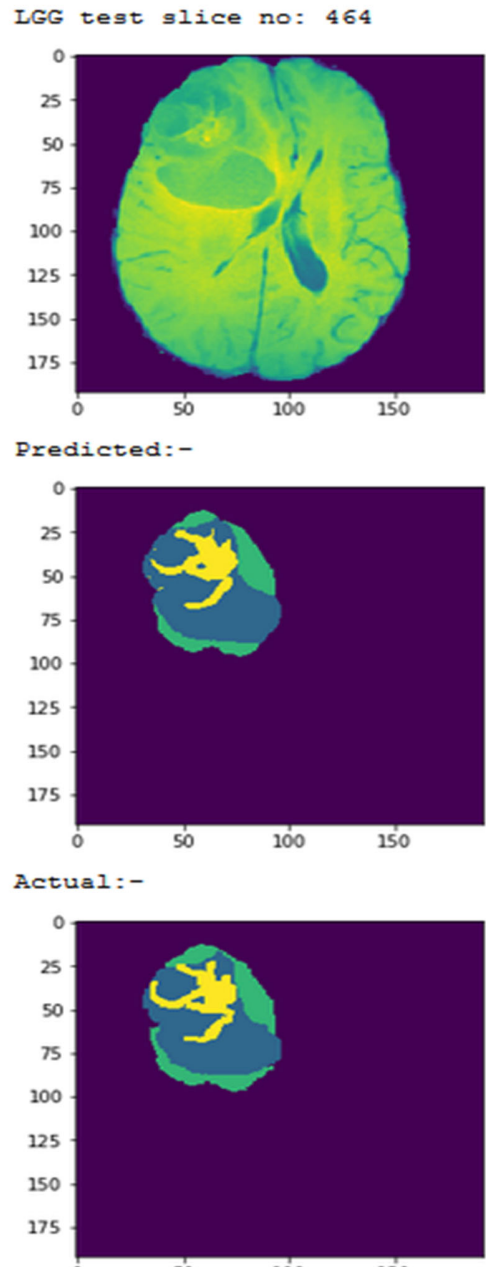


Fig. 6 LGG Test Slice 464 Pictorial results for the normal, predicted by the proposed system and actual (ground truth).

### 5.3 Evaluated Results

Dice Coefficient and Dice Coefficient Loss Function are most used to check the image segmentation accuracy. The formal definition of the Dice Coefficient is shown in the given equation no (1).

$$\text{Dice Coefficient} = \frac{2|X \cap Y|}{|X| + |Y|} \quad (1)$$

By applying this equation, we can get the overlap values for the actual resultant image with the ground truth images. By applying this equation, we can get the overlap values for the actual resultant image with the ground truth images. This gives us an indication of the overlap of the images.

#### Model Loss Graph

The graph of the Dice Coefficient loss is shown in Figure 6, in which the training and validation datasets model loss is shown. As the number of epochs increases, the Dice Coefficients for the training and validation dataset decrease. This is because the Dice values are a maximum at the start of the epochs, and as the number of epochs increases, the dice values decrease, as shown in Figure 6. It means our proposed system is the best and gives good results.

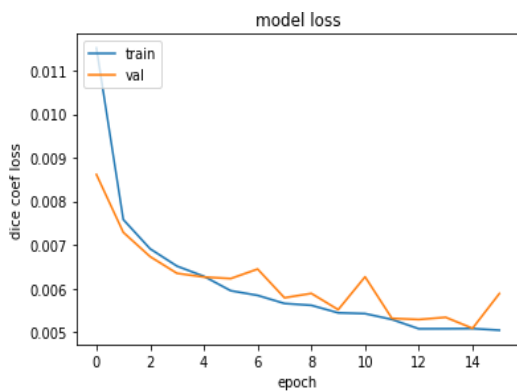


Fig. 6 Model Loss Graph for the Training and Validations data with Dice Coefficients and the epochs.

#### Model Score Graph

The model score graph, shown in Figure 7, shows the dice coefficient values against the training and validation datasets. The dice values improve by increasing the number of epochs, as shown in Figure 7.

The proposed system outperformed other brain tumor segmentation methods on the state-of-the-art BRATS 2018 dataset and the dice coefficient values for the test sets for both HGG and LGG, as shown in Table 1.

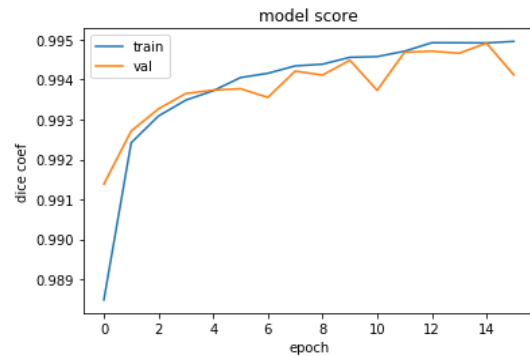


Fig. 7 Model Score Graph for the Training and Validations data with Dice Coefficients and the epochs.

After performing various experiments, we achieved the best Dice Coefficient for both the HGG and LGG data sets. The HGG volumes used for testing reached a maximum Dice Coefficient of 0.9855, with the LGG volumes Dice Coefficient being 0.9950. This is proof that our proposed model performs well.

Table 1. Proposed Model Test Sets with Dice Coefficient Values.

Test Samples	Test Sets	Dice Values
1	HGG Volumes Set-01	0.9795
2	HGG Volumes Set-02	0.9855
3	HGG Volumes Set-03	0.9793
4	LGG Volumes Set	0.9950

#### Comparison with state-of-the-art techniques

The proposed system technique is compared with state-of-the-art techniques under defined circumstances. MICCAI BRATS dataset is used in the proposed system and the state-of-the-art techniques. Dice value results are shown in Table 2. The dice values for the proposed system and state-of-the-art techniques clearly show our proposed system outperforms. Visual results and calculated results prove the proposed system's performance.

Table 2. Comparison with state-of-the-art techniques.

No	State-of-the-art Techniques	Dice Values
1	Mohammad A. Naser [15]	0.92
2	Chandan Ganesh [16]	0.86
3	Proposed System	0.99

The proposed system can accurately determine the size and structure of the tumor from an MRI. In addition, the Dice Coefficient shows that the proposed system performs well for the BRATS dataset.

## 6. Discussion

In this study, we proposed an automatic brain tumor segmentation system, which accurately addresses the tumor's localization and segments out the tumorous area. Compared with the already developed techniques, we employed the approach that segments the tumorous area with excellent dice values. Our proposed approach gives a solution by introducing pre-processing techniques for a large volume of data. Pre-processing steps were performed to make the NumPy array for further processing of data. These pre-processing techniques suggest dealing with a large volume of data. We trained our proposed system using the U-Net algorithm, which also takes more layers to get the high dimension outputs. We used the state-of-the-art BRATS 2018 dataset to evaluate our proposed system. Accurate tumor segmentation can be seen in Figures 2, 3, and Figure 4. These figures represent segmented tumor results for the HGG volumes. Figure 5 and Figure 6 show the visual results for the LGG volumes. The test data results for the proposed system in dice values are shown in Table 1. Dice values were obtained using the BRATS 2018 dataset, showing the best results for HGG and LGG volumes. This proposed system outperformed as compared to the state-of-the-art methods for brain tumor segmentation.

The proposed system fulfills all the requirements mentioned in the problem statement and meets the tumor segmentation for brain MRIs. Furthermore, this system properly addresses tumorous area localization with accurate segmentation.

## 7. Conclusion

Accurately brain tumor segmentation for the MRI in which different features affect different segmentation results. To compute the large volume of MRI data and accurately segment the proposed system. This system proposed pre-processing techniques to store and process a large amount of data. We used the U-Net with additional layers, which give high dimension outputs for the MRI. Furthermore, the Dice Coefficient values show that the proposed system has excellent results with maximum values obtained from the test datasets. We can use various other datasets like BRATS or other real-time datasets to improve the model scalability in future work.

## References

- [1] B. H. Menze et al., "The Multimodal Brain Tumor Image Segmentation Benchmark (BRATS)", *IEEE Transactions on Medical Imaging*, Vol. 34, No. 10, 2015, pp. 1993-2024.
- [2] U. A. Nayak, M. Balachandra, K. N. Manjunath, and R. Kurady, "Validation of Segmented Brain Tumor from MRI Images Using 3D Printing", *Asian Pacific Journal of Cancer Prevention: APJCP*, Vol. 22, No. 2, 2021, p. 523, <https://doi.org/10.31557%2FAPJCP.2021.22.2.523>
- [3] M. S. Felson, "Brain Cancer", *WebMD LLC*, 9 Oct 2019. [Online]. Available: <https://www.webmd.com/cancer/brain-cancer/brain-cancer>
- [4] M. Soltaninejad, G. Yang, T. Lambrou, N. Allinson, T. L. Jones, T. R. Barrick, F. A. Howe, and X. Ye, "Automated Brain Tumour Detection and Segmentation Using Superpixel-Based Extremely Randomized Trees in FLAIR MRI", *International Journal of Computer Assisted Radiology and Surgery*, Vol. 12, 2017, pp. 183-203, <https://doi.org/10.1007/s11548-016-1483-3>
- [5] Z. U. Rehman, S. S. Naqvi, T. M. Khan, M. A. Khan, and T. Bashir, "Fully Automated Multi-Parametric Brain Tumour Segmentation Using Superpixel Based Classification", *Expert Systems with Applications*, Vol. 118, 2019, pp. 598-613, <https://doi.org/10.1016/j.eswa.2018.10.040>
- [6] M. A. Khan, "Brain Tumor Detection and Classification: A Framework of Marker-based Watershed Algorithm and Multilevel Priority Features Selection," *Microscopy Research and Technique*, Vol. 82, 2019, pp. 909-922, <https://doi.org/10.1002/jemt.23238>
- [7] P. G. Rajan and C. Sundar, "Brain Tumor Detection and Segmentation by Intensity Adjustment", *Journal of Medical Systems*, Vol. 43, 2019, pp. 1-13, <https://doi.org/10.1007/s10916-019-1368-4>
- [8] H. Byale, G. M. Lingaraju and S. Shivasubramaniyan, "Automatic Segmentation and Classification of Brain Tumor Using Machine Learning Techniques," *International Journal of Applied Engineering Research*, Vol. 13, 2018, pp. 11686-11692
- [9] N. Nooshin and K. Miroslav, "Brain Tumors Detection and Segmentation in MR Images: Gabor Wavelet vs. Statistical Features", *Computers & Electrical Engineering*, Vol. 45, 2017, pp. 286-301, <https://doi.org/10.1016/j.compeleceng.2015.02.007>
- [10] "Multimodal Brain Tumor Segmentation Challenge 2018", *Section for Biomedical Image Analysis (SBIA): Perelman School of Medicine*, 16 Sep 2018. [Online]. Available: <https://www.med.upenn.edu/sbia/brats2018/data.html>.
- [11] J. Jordan, "An Overview of Semantic Image Segmentation", *Machine Learning Blogs*, 21 May 2018. [Online]. Available: <https://www.jeremyjordan.me/semantic-segmentation/>
- [12] M. P. Starmans, S. R. van der Voort, J. M. C. Tovar, J. F. Veenland, S. Klein, and W. J. Niessen, "Radiomics: Data Mining Using Quantitative Medical Image Features", *Handbook of Medical Image Computing and Computer Assisted Intervention*, pp. 429-456, Academic Press.



- [13] R.A. Zeineldin, M. E. Karar, J. Coburger, C. R. Wirtz, and O. Burgert, "DeepSeg: Deep Neural Network Framework for Automatic Brain Tumor Segmentation Using Magnetic Resonance FLAIR Images", *International Journal of Computer Assisted Radiology and Surgery*, Vol. 15, No. 6, 2020, pp.909-920, <https://doi.org/10.1007/s11548-020-02186-z>
- [14] O. Ronneberger, P. Fischer, and T. Brox, "U-net: Convolutional Networks for Biomedical Image Segmentation", *International Conference on Medical Image Computing And Computer-Assisted Intervention*, pp. 234-241, Springer, Cham.
- [15] M. A. Naser, and M. J. Deen, "Brain Tumor Segmentation and Grading Of Lower-Grade Glioma Using Deep Learning in MRI Images", *Computers in Biology and Medicine*, Vol. 121, 2020, p. 103758, <https://doi.org/10.1016/j.compbiomed.2020.103758>
- [16] C. G. B. Yogananda et al, "A Fully Automated Deep Learning Network for Brain Tumor Segmentation", *Tomography*, Vol. 6, 2020, pp. 186-193, <https://doi.org/10.18383/j.tom.2019.00026>